Light Metals 2013 *Edited by: Barry Sadler*
TMS (The Minerals, Metals & Materials Society), 2013

IMPACTS OF IMPURITIES INTRODUCED INTO THE ALUMINIUM REDUCTION CELL

J.B.Metson[1,2,3], D.S.Wong[1], J.H.Hung[1], and M.P.Taylor[1,4]
[1]Light Metals Research Centre, [2]School of Chemical Sciences, [3]MacDiarmid Institute for Advanced Materials and Nanotechnology.
[4]Department of Chemical and Materials Engineering,
The University of Auckland, Private Bag 92019, Auckland 1142. New Zealand

Keywords: Aluminium electrolysis, Impurities, Alumina solubility,

Abstract

Impurities enter the aluminium reduction process largely through raw materials and operational practices. The declining quality of petroleum cokes, and the steadily increasing efficiency in the capture and recycle of pot fumes, increases impurity burdens with consequent impacts on cell performance and metal quality. Aluminas are a key and quite variable impurity source, with little incentive for producers to drive purity improvements. Beyond metal quality, the critical impacts lie in pot operations where control, or even analysis, of bath chemistry becomes increasingly problematic. Impurities have measureable impacts on current efficiency, and on anode effects, driven by inability to efficiently dissolve alumina. Impurity reduction strategies have been driven by perceived problem elements, for example phosphorus, however these processes generally entail an unacceptable level of collateral alumina loss. It is clear that the alumina contributions to impurity burdens and electrolyte chemistry, are increasingly complex and impact on the way reduction cells are operated.

Introduction

The target of aluminium production has always been the production of a sufficiently pure metal to meet market demand, at a cost which allows the smelter to operate profitably. Thus at a fundamental level, the introduction of impurities into the smelting process and their transfer into the product metal, defines the first of these objectives, while the effects of impurities on the efficiency of production impact on the latter consideration. Iron might be a typical example of the former, while phosphorus can be viewed in the latter category due to its effects on the current efficiency of the process [1].

The key medium through which all impurity transport takes place is the electrolyte. Thus it is worth considering in some detail the pathways of impurities through the electrolyte and the mechanisms, in as much as they are known, by which impurities are directed into these pathways. Impurities transit through the electrolyte and partition between the duct and the metal, with widely differing efficiencies, however there have been relatively few mass balance type studies that have addressed overall impurity sources and sinks and it is clear that these are highly technology specific. What is also apparent is the lack of any recent data on partition factors reflecting the distribution between metal and duct for modern large cell technologies.

A survey of impurity studies over time indicates that as cell technology has converged on increasingly closed (good crust integrity, well hooded), point fed cells supported by effective fume capture and dry-scrubbing, the impurity burden reporting to the metal has increased. This is as anticipated, but when coupled with increasing input loads, for example due to rising impurities in petroleum cokes, then metal grades become progressively harder to meet.

Unless there is a volatile or particulate loss pathway, elements with reduction potentials larger than that of aluminium should accumulate in the electrolyte. However the impacts of activity profiles near the metal pad/electrolyte interface may indeed allow activities to approach that of Al and thus the reduction of some of these impurities and accumulation in the metal becomes possible. Tabereaux [2] outlines how sodium accumulation can thus be used as a proxy for current efficiency. Similar logic suggests elements with lesser reduction potentials than aluminium should largely be reduced and report to the metal.

The assumption has frequently been made that most impurity species do not approach solubility limits in the electrolyte, although it is not clear that this is the case, particularly for heavily modified electrolyte chemistries, where impurity behavior becomes much more complex.

Previous studies of impurity distributions

Irrespective of the pathway by which they are introduced, impurities invariably pass through the electrolyte and interact with it. From the bath they then partition to report either to the metal, to the electrolyte, or are ejected into the duct. For the overwhelming proportion of smelters, any condensed or particulate emissions into the duct will then be captured in the dry-scrubber and returned to the cell with the secondary alumina. However if there is the option of controlling alumina distribution then a smelter may choose to redistribute these impurities by feeding some cells with primary alumina and concentrating impurities into the rest of the reduction cells.

Thus there is significant interest in impurity partitioning, despite the limited data on partition ratios for current technologies. Early work modeling the transfer of impurities has been mostly related to predicting the impacts of fume scrubbing. A volatility distribution factor (α) quantifying the partition of various impurity into the gas stream was therefore defined [3], where:

$$\alpha = \frac{Impurities\ in\ Pot\ Gas}{Impurities\ in\ Raw\ Materials}$$

Taking into account major process material output streams other than metal and duct emissions, which includes anodes and the cover removed with the butts (if these materials are not feed back into the bath), Zhang et al. [4] defined the metal and duct/gas partition factors as:

$$\frac{duct}{feed}factor = \frac{Impurity\ in\ duct}{Impurity\ in\ Net\ Feed} \qquad \textbf{Equation 1}$$

$$\frac{metal}{feed}factor = \frac{Impurity\ in\ Metal}{Impurity\ in\ Net\ Feed} \qquad \textbf{Equation 2}$$

Where 'impurity in net feed' is the impurity in the total process feed minus any output of process materials excluding metal and duct emissions (i.e. net feed = impurity in metal + impurity in duct). These two partition factors can be related by the equation:

$$\left(\frac{\text{duct}}{\text{feed}}\text{factor}\right) = 1 - \left(\frac{\text{metal}}{\text{feed}}\text{factor}\right) \qquad \textbf{Equation 3}$$

Partitions factors (metal/feed) obtained from various literature sources can be found in Table 1. These are converted from reported α factors using Equation 3, or calculated from output metal and duct impurity values using Equation 2. These factors are then plotted over time in Figure 1. As can be seen, partition factors from different sources can be widely variable, as they are technology sensitive, and are also affected by factors such as cell operation, control strategy and maintenance. Of the impurity elements listed in Table 1, vanadium data is especially scattered. This is attributed by Zhang et al. [4] to the difficulties in accurate analysis of vanadium in the duct emission streams.

Table 1: Partition factors for impurity distributions (metal/feed)

	Tech1 [3]	Tech2 [4]	Tech3 [5]	Tech4 [6]	Tech5 [6]	Tech6 [2]
			Ardel	High purity trial	Avg. 12 references	NZAS
	Erftwerk		HAL-150			P69
	SW/BB		PF			CW/BB
	CPA		Pre-Bake			Pre-Bake
	125kA	140kA	150kA			150kA
	(1973)	(1976)	(1978)	(1988)	(1988)	(1996)
Ti	0.379	0.430			0.500	0.763
Fe	0.544	0.580	0.700	0.595	0.870	0.814
Ga	0.496		0.750	0.658	0.660	0.761
Si	0.918	0.930		0.952	0.950	0.980
P	0.143				0.090	
V	0.345	0.150	0.800	0.167	0.390	0.493
Ni		0.600	0.090	0.103	0.330	
Zn	0.800				0.660	
Cu			0.180		0.550	
Pb			0.320		0.560	
Mn					0.920	
Cr					1.000	

SW – Side Worked PF – Point feed
BB – Bar Breaker CW – Centre worked
CPA – Continuous pre-bake anode

The partition factors in Figure 1 suggest considerable scatter across a range of technologies, overlaid on a general improvement in "closed cycle" operations as impurities are more effectively captured in the process with improved technology and operating practice. The data in Table 2 and Figure 2 reflect similar trends over time for a single technology.

Table 2: Published Partition factors (metal/feed) calculated using data from Slovalco. for iron [9], vanadium[10], and phosphorus [11]. - side-riser, point-feed PB cells.

	Partition Factor (metal/feed) [9,10,11]							
	1997	**1998**	**1999**	**2000**	**2001**	**2002**	**2003**	**Avg**
Fe		0.66	0.80	0.77	0.83	0.87		0.79
V					0.95	0.98	0.99	0.97
P	0.06	0.09	0.17					0.11

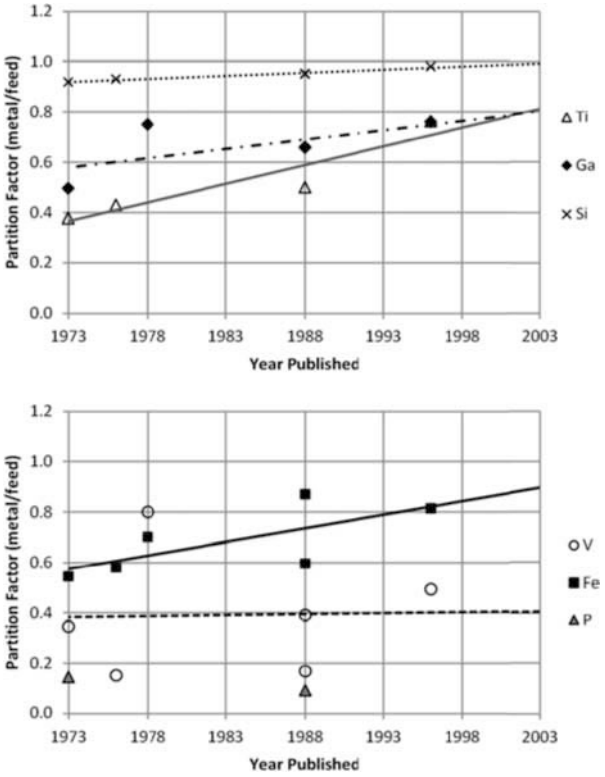

Figure 1: Partition factors (metal/feed) taken from Table 1 for selected impurities.

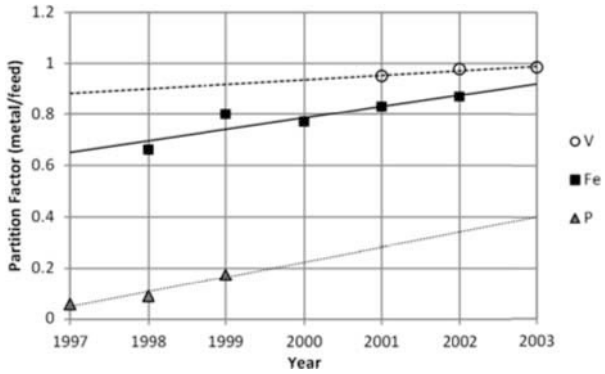

Figure 2: Graph showing the increase of partition factor (metal/feed) of various impurities for a single smelter (see Table 2).

However such comparisons also assume a stable input burden. If impurities have reached an equilibrium solubility limit in the

electrolyte, then an increasing raw material impurity input burden would have a similar impact in increasing the apparent partitioning into the metal. Cole et al. [12] report the impact on metal quality of increasing Fe in raw materials over time, and note that other impurities and vanadium in particular, closely follow the increase in metal Fe levels. This is significant as the dominant source of Fe lies in the alumina where the impurity levels increased over the period studied, while V is predominantly sourced from the anode coke where V content had not increased. The study confirmed this behavior with deliberately introduced impurities and highlights the coupled behavior, suggesting such a bath solubility limit. This also indicates the central role of transit through the electrolyte in dictating impurity pathways.

Goodes [8] carried out a comprehensive study of the partitioning of impurities between electrolyte, metal and duct. The work includes both plant studies across several technologies and laboratory simulations, but concentrates on those impurities which impact on metal quality, rather than elements which impact on electrolyte chemistry. Impurity "volatility" factors suggest Ni and perhaps V are the only elements where volatility (as determined by loss from the electrolyte) is significant, although no transport mechanism is confirmed. Impurity transport is one way, with no partitioning from metal to bath observed. This is confirmed in rocking furnace trials without electrolysis and again supports the existence of a solubility limit in the electrolyte. Goodes proposes the existence of stable, non-reduced, impurity complexes in the electrolyte, although as pointed out, if these are simple fluoride species, thermodynamics favours transfer into the metal.

The common conclusion from a number of such transport studies is that there is almost no evidence for the direct volatilization of impurity rich phases capable of sufficient impurity transport to justify the partition factors observed. There is thus wide support for particulate based transport mechanisms with several authors identifying carbon particles as the major transport vector [13,14]. As cells become increasingly closed with point feeders and high crust integrity, the opportunities for particulate transport become more limited.

The impacts of electrolyte chemistry

From the considerations above, the central role of the electrolyte in impurity transport is clear, yet this is an area where there is still limited knowledge of impurity behavior. Debate over the role of solubility of impurities in the molten salt electrolyte has extended over many years with theoretical approaches limited by the difficulty of including all the species which accumulate in the industrial electrolyte and experimental approaches limited by working with electrolytes often not representative of the current industrial situation.

Once they enter the electrolyte and dissolve, on the basis of reduction potentials, we might expect many of the impurity metals entering the cell through anode carbon or alumina to quantitatively report to the metal. That they do not is apparent in the partition factors outlined above (Table 1). Thus it is necessary to argue for stable complexation of, for example, V and Ti in the electrolyte and a concentration which rapidly accumulates to an equilibrium value. Once such an equilibrium limit is reached then we expect to observe the collective behavior above where Fe and V levels in the metal are coupled [12].

We would also expect any such solubility limit to be particularly sensitive to the specific chemistry of the electrolyte. In addition to the excess AlF_3, Al_2O_3 and CaF_2 normally found in conventional cryolite-based electrolytes, the effect of these modifiers LiF, MgF_2, KF has been studied extensively in the past 50 years [15]. There is now a reasonable level of understanding on the effects of these additives on operations (liquidus temperature, alumina solubility, current efficiency, etc). However many of these studies have focused on simplified binary, ternary or even quaternary bath systems [16] as opposed to the emerging complex systems that combine all of these modifiers.

The global trends in rising coke impurities have been well documented [17,18], however the trends in alumina impurities, particularly in the most rapidly expanding areas of production, are more complex. Feng Niaxiang et al. [19] comment on the impacts of alumina impurities in modifying bath chemistry and thus on cell performance, in high amperage Chinese technologies. Although the impacts on interfacial surface tension and thus on current efficiency are highlighted, little comment is made on impacts on cell performance or impurity transport arising from alumina solubility changes. Table 3 below, reproduced from that paper, indicate the particular impurities that dominate this bath chemistry modification.

Table 3. Impurities in alumina's from Henan province (%) [19].

	Li	K	Ca	α-Al_2O_3
Zhongzu	0.014	0.052	0.02	2.5
Wanji	0.084	0.019	0.02	1.4
Kaiman	0.039	0.0001	0.037	2.4
Easthope	0.053	0.022	0.035	3.8
Xiangjiang Wanji	0.073	0.015	0.020	1.2
Yixiang	0.040	0.018	0.021	0.9

These complex bath chemistries are becoming more common in the Chinese smelting community. As indicated above, the modifiers LiF, MgF_2 and KF are often appearing in electrolytes – largely as a result of the alumina impurities in Table 3, as opposed to active additions by smelters themselves. Many of these facilities are subject to significant variations in impurity levels from incoming alumina streams, particularly those with limited ability to 'pick and choose' their alumina sources. This is illustrated by a survey of LiF and MgF_2 levels (wt %, by wet chemistry) across four potlines at one Chinese smelter. As shown in Figure 3, average modifier levels have varied significantly over 8 years, purely as a result of varying impurity inputs from alumina. While not shown, KF is another impurity that needs to be accounted for (typical levels of 2% wt at this smelter).

The impurities identified in Table 3 would all be expected to accumulate in the electrolyte and thus the combination and variation of these modifiers over time has major impacts on the control of the reduction cell. Although the cumulative impact is to reduce liquidus temperature and thus operating temperature, the impacts on current efficiency, driven by interfacial surface tension and on alumina dissolution are more complex. These are discussed in more detail below.

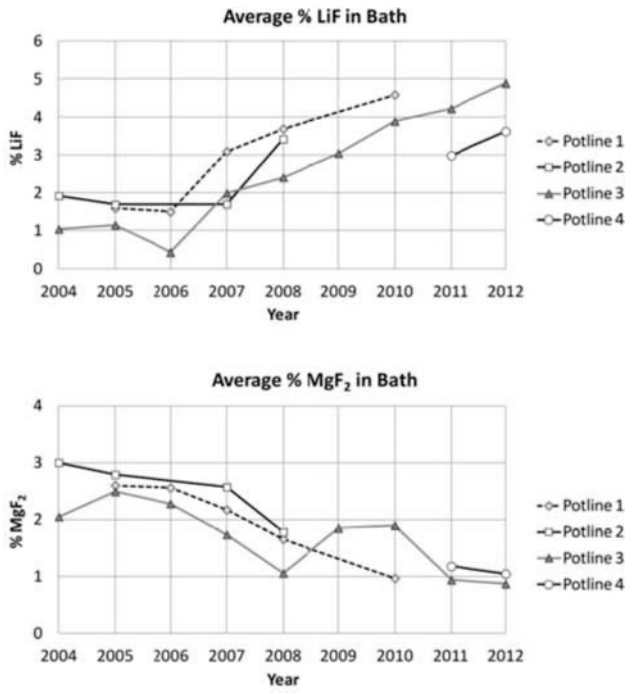

Figure 3: Variations with time in % levels LiF [Top] and MgF_2 [Bottom] impurities in heavily modified baths at one smelter.

Alumina Solubility

Models on the effect of bath modifiers on alumina solubility have been developed by a number of investigators, the most commonly used being Skybakmoen's [20] empirical correlation. This accounts for varying levels of excess AlF_3, CaF_2, LiF and MgF_2, but not KF. In another study, Fernandez *et al.* [21] modeled the impact of KF in a ternary Na_3AlF_6-KF-Al_2O_3 system. The former suggests that LiF and MgF_2 modifiers generally *reduce* alumina solubility, whereas the latter suggests that KF tends to *increase* alumina solubility. To examine the combined effect of these modifiers, Skybakmoen and Fernandez' correlations were combined [22], resulting in the following equation for alumina saturation (bath modifier levels in wt %):

$$[Al_2O_3]_{sat} = A\left(\frac{t}{1000}\right)^B + 0.16[KF] - 1.24\times10^{-3}[KF]^2 \qquad (1)$$

where t is temperature (°C) and

$$A = 11.9 - 0.062[AlF_3] - 0.0031[AlF_3]^2 - 0.50[LiF] - 0.20[CaF_2] - 0.30[MgF_2] + \frac{42[LiF]\cdot[AlF_3]}{2000 + [LiF]\cdot[AlF_3]}$$

$$B = 4.8 - 0.048[AlF_3] + \frac{2.2[LiF]^{1.5}}{10 + [LiF] + 0.001[AlF_3]^3}$$

Using equation (1) and Solheim's liquidus equation [23], bath liquidus vs. alumina concentration curves can be drawn for conventional and heavily-modified bath chemistries, as shown in Figure 4. Bath 'A' represents conventional Western bath, as defined by Frolov [22]; bath 'B' is an example of heavily modified baths found at one Chinese smelter; finally, bath 'C' represents a modified bath with high KF (also investigated by Frolov [22]).

For each of these chemistries, an operating temperature (based on liquidus with a 3% Al_2O_3 target and 10°C superheat) and alumina solubility were estimated, as shown in Table 4. Compared to conventional bath (A) therefore, the combined effect of high modifier levels in Chinese bath (B) results in a significant *degradation* in alumina solubility. In addition, the lower operating temperatures encountered with highly-modified bath act to further reduce alumina solubilities.

While increasing KF levels in modified baths (C) may help increase alumina solubility, the lower operating temperatures counter this effect somewhat; furthermore, high levels of KF are undesirable due to negative effects on cathode life.

Reduced alumina solubilities in these highly modified baths pose a significant issue for emerging cell technologies particularly in China. Many of these are veering towards high amperage, low ACD operations with increasing anode sizes and cell dimensions. With such trends, the transport of alumina from the electrolyte surface to the anode-cathode gap (and therefore maintaining sufficient concentrations to prevent anode effects) is likely to be an increasing problem. The recent finding of 'continuous PFCs' (those not related to anode effects) [24,25] and the presence of many short-lived, 'self-terminating' anode effects (i.e. terminate without manual or automatic intervention) in many of these smelters may well be symptoms of these issues.

Bath Chemistry	wt%	[AlF_3]	[CaF_2]	[LiF]	[MgF_2]	[KF]
A - Conventional		10.1	6	0	0.5	0
B - Modified Chinese		7.5	5	4.5	1	2
C - Modified High KF		4.3	4	2.1	1.2	4.7

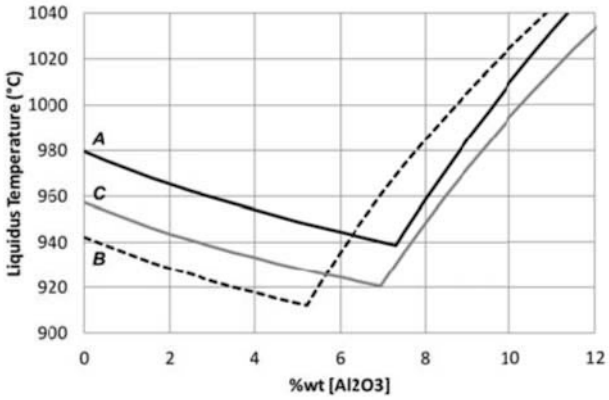

Figure 4: Liquidus temperature vs. alumina solubility (wt %) in a complex Na_3AlF_6-AlF_3-Al_2O_3-CaF_2-LiF-MgF_2-KF system for three different bath chemistries.

Table 4: Alumina solubilities with different bath chemistries, operating at 10°C superheat (in bath with 3% wt Al_2O_3 in the bulk electrolyte)

Bath Chemistry	Operating T (°C)	$[Al_2O_3]_{sat}$
A – Conventional	969.3	8.4 %
B – Modified Chinese	932.7	5.9 %
C – Modified High KF	948.0	8.0 %

Impact on Heat Balance & Bath Chemistry Control

High levels of electrolyte modifiers (LiF, MgF_2, KF) have considerable impacts on the control of bath chemistry and cell heat balance. Since these modifiers are not present as controlled additions to the process, their effects on cell liquidus temperature forces smelters to change operating targets. Where modifier levels vary significantly over time (as per Figure 3), smelters must adjust either liquidus and operating temperatures (while maintaining constant % excess AlF_3), or adjust their operating % excess AlF_3 (to maintain the same liquidus and operating temperature).

Varying levels of bath modifiers pose another significant issue in the area of bath chemistry control, where AlF_3 additions are scheduled to maintain consistent bath chemistry and hence liquidus temperatures. X-Ray Diffraction (XRD) methods are the most commonly used technique for analyzing routine bath chemistries. However, many of these methods (e.g. Potflux) have been designed for conventional Western baths (Na_3AlF_6-Al_2O_3-CaF_2 systems), and are not easily adapted for more complex bath chemistries. Heavily modified baths, such as many of those in China, require accounting for Li, Mg and K-based cryolites (Na_2LiAlF_6, K_2NaAlF_6 and Na_2MgAlF_7) in order to obtain an accurate measure of bath ratio or % excess AlF_3; however adjusting traditional XRD techniques to accommodate these compounds is not a trivial matter. New XRD hardware and techniques (high speed detectors, with Rietveld analysis) do provide advantages in accounting for these modifiers, but require significant capital investment on the part of the smelter.

In recent years, a number of smelters have replaced traditional XRD bath chemistry analyses with liquidus/superheat probes (e.g. Hereaus, STAR), which are expected to take into account the effect of all modifiers for bath chemistry control. However, to our knowledge, a least one smelter (with heavily modified baths) has reported difficulties in obtaining clear liquidus transition points with these probes, perhaps as a result of non-conventional liquidus transitions and bath phases.

Conclusions

Impurities enter the aluminium reduction process through raw materials and operational practices. In terms of the impurity burden, the smelter typically operates largely as a closed cycle and thus although there may be opportunity to redistribute impurities, the metal produced is the ultimate sink for most of the metallic impurities introduced. The key to such redistribution lies in the partitioning of impurities between metal and duct, with passage through the electrolyte the key to exploiting this segregation.

However impurity impacts lie well beyond metal quality with the modification of electrolyte chemistry an increasingly important factor in some areas of the world. In China, in particular, the dramatic increase in smelting capacity, coupled with alumina compositions relatively rich in the alkaline and alkaline earth metals, is changing the range of electrolyte chemistry and conventional operating parameters. Computations of liquidus temperatures and superheats are significantly impacted by these changes, with more subtle changes in alumina solubility and that of reducible impurities. Both are typically reduced in these modified bath chemistries, introducing further challenges in cell operation, but quantitative analysis of likely impacts is difficult.

Acknowledgements

The skilled assistance of Tanya Groutso and Nursiani Tjahyono in the analysis of bath samples is acknowledged and funding support at various stages of our impurities studies has been provided by New Zealand Aluminium Smelters Ltd, BP Coke, Rain CII Carbon and Hydro Aluminium.

References

1. Hauglan E., Haarberg G. M.Thisted E. and Thonstad J. TMS Light Metals, 2001, J Anjier Ed. p.549-553 (2001).
2. Taberaux A.T. TMS Light Metals, W. Hale, Ed. p.319-326, (1996)
3. Goodes, C.G. and S.H. Algie, TMS Light Metals: P Campbell Ed. p. 199-207. (1989)
4. Zhang, W., Liu X. McMaster P., and Taylor M. TMS Light Metals 1996: W.Hale Ed. p. 405-411. (1996)
5. Sparwald, V., Erzmetall, **26**(11): p. 529-33. (1973) .
6. Frankenfeldt, R.E. and U. Mannweiler, Erzmetall, **29**(3): p. 130-133. (1976).
7. Thonstad, J., Nordmo F. and Roseth S. TMS Light Metals, 1978 **2**: p. 463-479. (1978)
8. Goodes, C.G., PhD Thesis, University of Queensland. (1988).
9. Šimko, F. Daněk V. and Stas M. Metallurgical and Materials Transactions A, **37**(3): p. 731-738. (2006)
10. Daněk, V., et al.,. Ind. Eng. Chem. Res., 2004. **43**(26): p. 8239–8243.
11. Danek, V., et al. Eleventh International Aluminium Symposium. 2001. Trondheim-Bergen-Trondheim.
12. Cole D., Terrell M., Wood S. TMS Light Metals 1996. J. Evans Ed. p. 1996.
13. Liu, X. Clements I. and George S. Australasian Smelting Technology Workshop p.457, (1992).
14. Metson J B. Proceedings of the Ninth International Symposium on Light Metals Production. J.Thonstad Editor. p.259-264. (1997).
15. Kvande, H. JOM, p. 22-28, 1994.
16. Grjotheim, K., et al. Aluminium Electrolysis – Fundamentals of the Hall-Héroult Process, 2nd ed, Aluminium-Verlag, Düsseldorf, 1982.
17. Mannweiler U. Fischer W.K., Perruchoud R. TMS Light Metals 2009. G. Bearne Ed. p. 909-911 (2009).
18. Grandfield J.F. and Taylor J.A. TMS Light Metals. 2009. G.Bearne, Ed. p. 1007-1011 (2009)
19. Feng Niaxiang, Peng J., Wang, Y. Di Y., You J., Laio X. TMS Light Metals. 2012. C. Suarez Ed. p. 563-568, (2012).
20. Skybakmoen, E., A. Solheim, and Å. Sterten. Metall. Mater. Trans. B., 28B, p.81-86, 1997.
21. Fernandez, R., K. Grjotheim and T. Østvold. TMS Light Metals, 1985. p.501-506, (1985)
22. Frolov, A.V., Gusev A.O., Zaikov Y.P., Kharmov A.P. Shurov N.I. Tkacheva O.Y. Apisarov A.P and Kovrov V.A. TMS Light Metals, 2007. M.Sorlie Ed. p.571-576, (2007).
23. Solheim, A., Rolseth S., Skybakmoen E., Stoen L. Sterten A. and Store T. Metall. Mater. Trans. B., 27B, 739-744, (1996).
24 Li, W., Zhao Q., Yang J., Qiu S., and Chen X. TMS Light Metals. 2011. S. Lindsay Ed. p.309-314, (2011).
25. Marks, J. and C. Bayliss. TMS Light Metals, 2012, C. Suarez Ed. p.805-808, (2012).